The Journal of Chemical Physics ARTICLE scitation.org/journal/jcp

Comparison of dynamic corrections to the quasistatic polarizability and optical properties of small spheroidal particles

Cite as: J. Chem. Phys. 156, 104110 (2022); doi: 10.1063/5.0085687
Submitted: 18 January 2022 • Accepted: 21 February 2022 •
Published Online: 14 March 2022

Matt R. A. Majić, Baptiste Auguié, and Eric C. Le Ru[a)]

AFFILIATIONS

The MacDiarmid Institute for Advanced Materials and Nanotechnology, School of Chemical and Physical Sciences, Victoria University of Wellington, P.O. Box 600, Wellington 6140, New Zealand

Note: This paper is part of the JCP Special Topic on Advances in Modeling Plasmonic Systems.
[a)]**Author to whom correspondence should be addressed:** eric.leru@vuw.ac.nz

ABSTRACT

The optical properties of small spheroidal metallic nanoparticles can be simply studied within the quasistatic/electrostatic approximation, but this is limited to particles much smaller than the wavelength. A number of approaches have been proposed to extend the range of validity of this simple approximation to a range of sizes more relevant to applications in plasmonics, where resonances play a key role. The most common approach, called the modified long-wavelength approximation, is based on physical considerations of the dynamic depolarization field inside the spheroid, but alternative empirical expressions have also been proposed, presenting better accuracy. Recently, an exact Taylor expansion of the full electromagnetic solution has been derived [Majic *et al.*, Phys. Rev. A **99**, 013853 (2019)], which should arguably provide the best approximation for a given order. We here compare the merits of these approximations to predict orientation-averaged extinction/scattering/absorption spectra of metallic spheroidal nanoparticles. The Taylor expansion is shown to provide more accurate predictions over a wider range of parameters (aspect ratio and prolate/oblate shape). It also allows us to consider quadrupole and octupole resonances. This simple approximation can therefore be used for small and intermediate-size nanoparticles in situations where computing the full electromagnetic solution is not practical.

I. INTRODUCTION

The optical properties of sub-wavelength nanoparticles of noble metals are an important subject of study due to their ability to sustain strong plasmonic resonances in the visible and near infra-red regions. These localized plasmon resonances have found a range of practical applications, including refractive index sensing,[1] surface-enhanced Raman spectroscopy,[2–4] molecule/plasmon coupling studies,[5–8] thermoplasmonics,[9] and solar cell absorption enhancement.[10] General numerical approaches for calculating the optical properties of metallic nanoparticles[11] include the discrete dipole approximation,[12] the surface integral equation,[13,14] the finite-element method,[15] or the T-matrix method.[16,17] They are, however, computer-intensive, time-consuming, and/or relatively complex to implement. Mie theory[18] provides a relatively simple and efficient alternative but is only applicable to spherical nanoparticles. To understand the effects of non-spherical particle shapes on their optical properties, the spheroid geometry is a typical model system for which simple results can still be derived. The electromagnetic response of a small spheroidal particle can thus be derived within the quasistatic/electrostatic approximation (ESA),[2,18] where the incident electric field is considered homogeneous over the extent of the particle (but still varies in time). The validity of this approximation is, however, very limited, typically to sizes below $\sim\lambda/60$, where λ is the excitation wavelength in the incident medium. Much work has therefore been devoted to developing better approximations that extend this range of validity to sizes relevant to experimental work, typically between 20 and 100 nm.[19–26] Such approximations are typically expressed as a series expansion of the polarizability in terms of its size parameter, the product of the particle's size, and wavenumber. Most approximations only consider the first three terms of the dominant dipolar response.

While such a third order expansion with respect to particle size for small ellipsoidal particles was derived by Stevenson in

1953,[27] the results were too complex for most practical use. Instead, physicists have since looked at alternative approaches to find various corrections to the electrostatic polarizability. These derivations rely either on physical assumptions, such as a uniform but phase-varying internal field to derive a so-called dynamic correction to the polarizability,[19–21] or on empirical data[22,25,28] from fully numerical calculations. It should be noted that many of these efforts do not apply to oblate spheroids and/or do not reduce to the correct expressions in the spherical limit. Despite their shortcomings, these approximations are in great demand. For example, they have been applied to spheroidal nano-shells,[29] to study the resonance conditions of localized surface plasmon resonances,[25] to design nano-particles to optimize optical absorption in spherical particles,[30] to study infrared resonance damping in nanowires,[31] or to predict the resonances of nanorods[32] and nanodisks.[33] Recently, the exact Taylor expansion of the rigorous solution for spheroids was derived in the T-matrix framework, which provides a general description of a scatterer's multipolar response.[24] This led to yet another expression for the dynamic correction to the quasistatic polarizability, which should prove more accurate than other approximations of the same order, as it is obtained via an exact Taylor expansion. Indeed, these modified dipolar polarizabilities were recently used to calculate the surface and orientation-averaged Raman enhancement factors for spheroids, where the accuracy was greatly improved over the electrostatic approximations,[34] and have been extended to the special case of absorbing media,[35] where it was also shown to perform much better than the modified long-wavelength approximation (MLWA).

Here, we rigorously compare this new Taylor-based approximation to popular alternative expressions by calculating the orientation-averaged extinction/scattering/absorption spectra of spheroidal nanoparticles and using the exact T-matrix results as benchmark. We show that the new expressions provide the best agreement over the widest range of geometrical and material parameters. Our Taylor-based approximation also includes the quadrupole and octupole interactions, which we show are necessary for intermediate-sized particles. The Taylor approximation provides simple formulas to study the plasmon resonances of such particles and their dipolar/multipolar nature.

II. DIPOLAR APPROXIMATION

We consider a prolate or oblate spheroid with semi-axes c along the rotation-symmetry axis z and a along x and y (half-width) and with permittivity ε_2 embedded in a homogeneous and non-absorbing medium of permittivity ε_1. All materials are assumed isotropic and non-magnetic. We denote the relative permittivity $\varepsilon = \varepsilon_2/\varepsilon_1$. For both prolate and oblate spheroids, we define the eccentricity $e = \sqrt{c^2 - a^2}/c$, allowing e to be imaginary for oblate spheroids $(a > c)$. The spheroid is illuminated by a plane wave with wavelength λ and the wavenumber in the incident medium $k_1 = 2\pi\sqrt{\varepsilon_1}/\lambda$. The electromagnetic scattering problem consists in solving for the internal and scattered electric field and deriving experimentally relevant quantities, such as absorption, scattering, and extinction cross sections. This problem can be solved semi-analytically using either vector spheroidal harmonics or the T-matrix/Extended Boundary Condition Method (EBCM).[16,36] The latter is particularly suited to computing orientation-averaged cross sections. Both techniques are substantially more complex than Mie theory for spheres and suffer from possible numerical instabilities.[37] They are therefore less suited to routine modeling, for example, in a real-time experimental context, or to be included as building blocks in more complex theoretical models. This is why many approximations have been proposed, in particular, for nanoparticles where the size is smaller than or comparable to the wavelength.

For a spheroid, it is convenient to define the size parameter as $X_{\mathrm{eq}} = k_1 r_{\mathrm{eq}}$, where $r_{\mathrm{eq}} = \sqrt[3]{a^2 c}$ is the radius of a sphere of equivalent volume. Note that the definition of the size parameter varies between studies (with some, for example, using $X_c = k_1 c$ or $X_a = k_1 a$). Our definition of X_{eq} is chosen to capture the range of validity of small-X approximations more generally. The simplest and most commonly used small-X approximation is the Rayleigh–Gans or quasi-static approximation, where the particle response is obtained by solving an electrostatics problem where the incident field is constant (but the dielectric function still depends on frequency). This approach often focuses on the dipolar term, yielding a polarizability tensor that describes the particle's response to an incident field along any incident direction, in the long-wavelength limit. It is convenient to write the polarizability elements as[2]

$$\alpha = 3\varepsilon_1 V \beta, \tag{1}$$

where V is the particle volume ($V = 4\pi a^2 c/3$ here) and β is an adimensional polarizability. For spheroids, the electrostatic solution can be derived using spheroidal harmonics and yields the following well-known formulas for the principal dipolar polarizabilities for axial and transverse exciting fields:[2,18]

$$\beta_w^0 = \frac{\varepsilon - 1}{3L_w(\varepsilon - 1) + 3} \tag{2}$$

for $w = x, y, z$, where L_w are the dipole depolarization factors,

$$L_z = \frac{1 - e^2}{e^2}\left[\frac{\operatorname{atanh}(e)}{e} - 1\right], \tag{3}$$

$$L_x = L_y = \frac{1 - L_z}{2}. \tag{4}$$

Note that most studies provide different expressions for prolate and oblate spheroids, but all our expressions are valid for both prolate and oblate spheroids, with the parameter e being purely imaginary in the oblate case. These expressions describe very concisely the two main dipolar plasmon resonances of metallic spheroidal nanoparticles. Unfortunately, this approximation has a very limited range of validity, typically for size parameters smaller than $X_{\mathrm{eq}} \approx 0.1$, which correspond to very small dimensions $(\lambda/60)$, clearly not sufficient for many metallic nanoparticles used in experiments.

To overcome this limitation, there have been multiple attempts to develop more accurate expressions for the polarizabilities, while retaining the dipolar approximation. These can be found across the literature with different notations and conventions and not always explicitly considering the case $\varepsilon_1 > 1$ (for example, immersed in water). We, therefore, summarize the most important ones using consistent notations.

All these approximations include the same $\mathcal{O}(X^3)$ term accounting for the radiative correction[38] to ensure energy conservation. They differ, however, in the $\mathcal{O}(X^2)$ term, and some also include a $\mathcal{O}(X^4)$ correction. They can all be concisely expressed in the following form:

$$\beta_w = \frac{\beta_w^0}{1 - \Omega_w (k_1 c)^2 - i\frac{2}{3}X^3\beta_w^0}, \tag{5}$$

with Ω_w being the only difference between the various approximations. In fact, this general shape of Taylor expansion applies to the polarizability of a small particle of any shape or material.[41] Note that taking $\Omega_w = 0$ corresponds to the electrostatic approximation with radiative correction (ESA-RC).

One of the first proposed approaches to find Ω_w is called the modified long-wavelength approximation (MLWA) and includes a $\mathcal{O}(X^2)$ term called dynamic depolarization[19,20,39] with

$$\Omega_z^{\mathrm{MLWA}} = \frac{a^2}{c^2}\beta_z^0, \tag{6}$$

$$\Omega_x^{\mathrm{MLWA}} = \frac{a}{c}\beta_x^0 \tag{7}$$

in our notations. This term is derived by considering the uniform polarization induced inside the particle by an applied electrostatic field, expanding the electrodynamic field of the induced dipole to third order in k_1 and adding it to the external wave. The $\mathcal{O}(X^2)$ prefactor was, in fact, derived for spherical scatterers, but this approximation has nevertheless been used for spheroids.[19,20] This approach was revisited more recently for spheroids, with the uniform polarization integrated over the spheroid volume.[21] This introduces new dynamic depolarization factors D_w, which are similar in form to the static factors L_w,

$$D_z = 1 + \frac{3}{4}\frac{1+e^2}{1-e^2}L_z, \tag{8}$$

$$D_x = D_y = \frac{a}{2c}\left[\frac{3}{e}\mathrm{atanh}(e) - D_z\right]. \tag{9}$$

Within this extended MLWA (EMLWA), the correction factors take the form

$$\begin{aligned}\Omega_z^{\mathrm{EMLWA}} &= D_z\frac{a^2}{c^2}\beta_z^0,\\ \Omega_x^{\mathrm{EMLWA}} &= D_x\frac{a}{c}\beta_x^0.\end{aligned} \tag{10}$$

More approximations involving fitting parameters are discussed in Ref. 21, but they apply only to the main (β_z) resonance of prolate spheroids.

The MLWA or EMLWA, although better than the Rayleigh–Gans approximation, also become inaccurate at relatively small size, but it has inspired other approximations where the dependence of Ω_w is obtained from exact numerical results and fitted to a simple analytic function. This alternative approach was first proposed by Kuwata *et* al.[22] who focused on the longitudinal (z) resonance of gold and silver prolate spheroids and found

$$\Omega_z^{\mathrm{K}} = -3\beta_z^0\left[\left(-0.4865L_z - 1.046L_z^2 + 0.8481L_z^3\right),\right. \tag{11}$$

$$\left. + (k_1 c)^2\left(0.019\,09L_z + 0.1999L_z^2 + 0.6077L_z^3\right)\right]. \tag{12}$$

Note that the second term in this expression corresponds to a $\mathcal{O}(X^4)$ correction. A similar approach was taken recently by Yu et al.,[28] which gave (again only for the z resonance of prolate spheroids)

$$\Omega_z^{\mathrm{Y}} = 3\beta_z^0\left[0.5593L_z - 0.1\left(\frac{a}{c}\right)^{2.53}(k_1 c)^2\right]. \tag{13}$$

One common feature of all these approximations so far is that Ω_z/β_z^0 is independent of the material properties (ε).

We have recently proposed an alternative approach,[24] where the exact Taylor expansion of the multipolar T-matrix solution was carried out rigorously to third order, resulting in a similar functional form for the approximate polarizabilities [Eq. (5)] with

$$\Omega_z^T = \frac{1}{5}\frac{\varepsilon - 2 - \varepsilon e^2}{1 + (\varepsilon - 1)L_z} + \frac{9}{25}e^2, \tag{14}$$

$$\Omega_x^T = \frac{1}{5}\frac{\varepsilon - 2 + 3e^2}{1 + (\varepsilon - 1)L_x} - \frac{12}{25}e^2. \tag{15}$$

These Taylor expansions were checked numerically using numerical derivations and should be consistent with the results of Stevenson[27] but dramatically simpler. In particular, the results in Ref. 27 are given as numerators (i.e., Taylor expansions of α), while it has since been realized that expressing them equivalently as denominators (i.e., Taylor expansions of α^{-1}) is much more accurate at predicting plasmon resonances. Moreover, expressions in terms of α^{-1} also appear naturally in formal treatments of the electromagnetic scattering problem, for example, using volume-integral equations.[40,41] The main difference between Eqs. (14) and (15) and the previous expressions is that the term Ω_w/β_w^0 depends non-trivially on the material (ε), which partly explains why the previous approximations are not as generally applicable. It may be possible to derive Ω_w via a method similar to the MLWA, but the approach would have to be extended in order to capture this material dependence.

We studied the accuracy of these approximations by comparing their predictions against exact T-matrix results computed with the SMARTIES codes.[17,42] Rather than considering fixed incidence directions separately, we focus on the orientation-averaged cross sections, where both longitudinal and transverse plasmon resonances are visible. Within the dipolar approximation, the cross sections are obtained directly from the polarizabilities as[24,35]

$$\langle C_{\mathrm{ext}}\rangle = \frac{4\pi k_1 r_{\mathrm{eq}}^3}{3}\mathrm{Im}\{\beta_z + 2\beta_x\}, \tag{16}$$

$$\langle C_{\mathrm{sca}}\rangle = \frac{8\pi k_1^4 r_{\mathrm{eq}}^6}{9}\mathrm{Im}\left\{|\beta_z|^2 + 2|\beta_x|^2\right\}. \tag{17}$$

For the Kuwata and Yu approximations, we simply take $\Omega_x^K = \Omega_x^Y = 0$ since no expressions are readily available. For transverse excitation, they become therefore equivalent to the electrostatic approximation with radiative correction only. To compare different particle sizes with a common scale, it is convenient to normalize all

cross sections by a geometric cross section to obtain adimensional extinction/scattering coefficients (efficiencies). For spheres, the geometric cross section is simply defined as πa^2, but for spheroids, several choices are possible. We here choose πr_{eq}^2, which results in coefficients

$$\langle Q_{\mathrm{ext}} \rangle = \frac{\langle C_{\mathrm{ext}} \rangle}{\pi r_{\mathrm{eq}}^2} = \frac{4X_{\mathrm{eq}}}{3} \mathrm{Im}\{\beta_z + 2\beta_x\}, \tag{18}$$

$$\langle Q_{\mathrm{sca}} \rangle = \frac{\langle C_{\mathrm{sca}} \rangle}{\pi r_{\mathrm{eq}}^2} = \frac{8X_{\mathrm{eq}}^4}{9} \mathrm{Im}\left\{|\beta_z|^2 + 2|\beta_x|^2\right\}. \tag{19}$$

In Figs. 1 and 2, we compare the predictions of these approximations to the exact T-matrix solution by calculating the

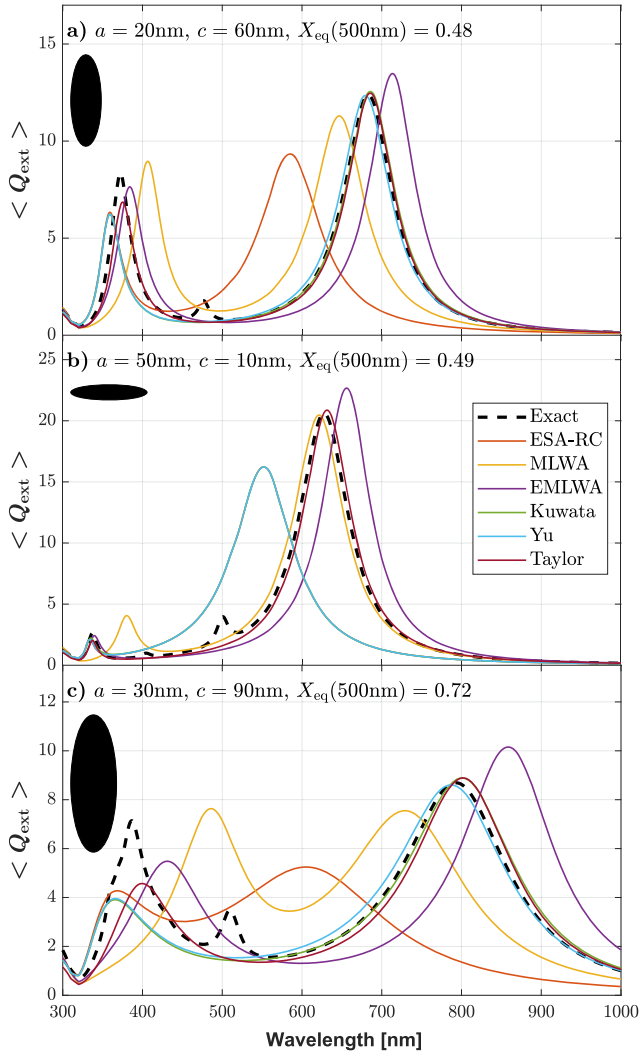

FIG. 1. Extinction coefficient spectra for silver spheroids of high aspect ratios calculated from the various approximations: (a) 40 × 120 nm^2 prolate, (b) 100 × 20 nm^2 oblate, and (c) 60 × 180 nm^2 prolate. The rigorous T-matrix reference solution is plotted as a dashed line. The size parameter X_{eq} is wavelength-dependent, and its value at 500 nm is indicated in each case.

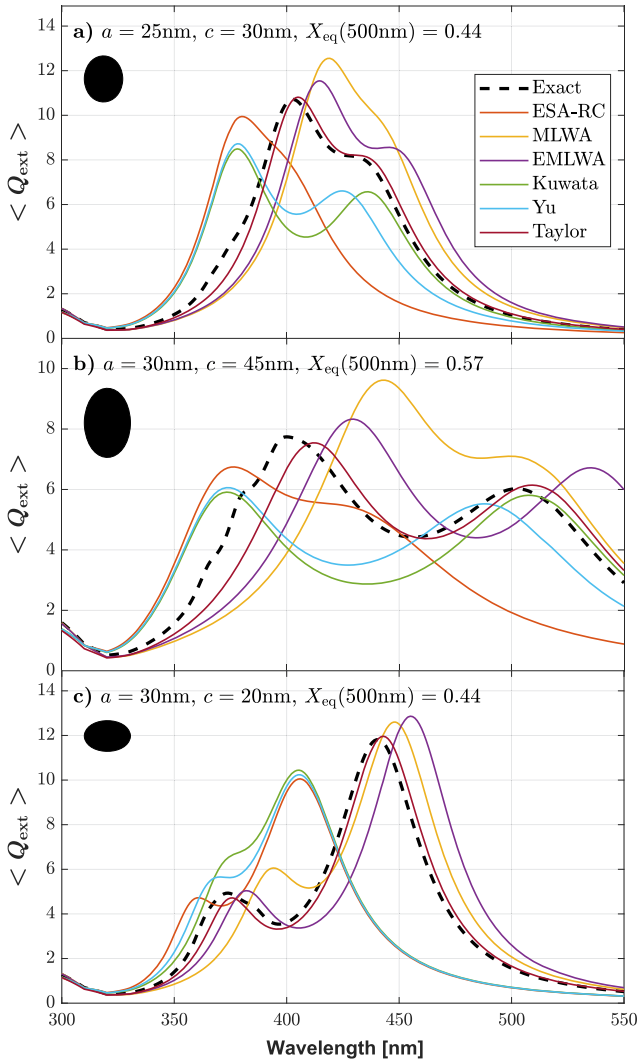

FIG. 2. Extinction coefficient spectra for silver spheroids of low aspect ratios calculated from the various approximations: (a) 50 × 60 nm^2 prolate, (b) 60 × 90 nm^2 prolate, and (c) 60 × 40 nm^2 oblate. The rigorous T-matrix reference solution is plotted as a dashed line.

orientation-averaged extinction spectrum of silver spheroids in water for a number of representative parameters: prolate and oblate spheroids of high (Fig. 1) and low (Fig. 2) aspect ratios with the size parameter in the range 0.4–0.7. The dielectric function for Ag was taken from Ref. 43 (B-corrected data). Similar figures were produced for gold spheroids in water and are given in Appendix A. The Kuwata, Yu, and Taylor approximations provide the best agreement for the z-dipolar resonance of prolate spheroids of intermediate to large aspect ratios. They are very good up to $X_{\mathrm{eq}} \sim 0.5$ and still reasonable at $X_{\mathrm{eq}} \sim 0.7$. The MLWA and EMLWA are clearly worse than these, but do provide some improvements over the simple ESA-RC. A similar comparison for oblate spheroids was made in Ref. 20. These plots also highlight several advantages of the Taylor approximation over Kuwata and Yu. First, it predicts with

good accuracy the transverse (x) resonance in contrast to all the other approximations. Second, it is applicable to oblate as easily as to prolate spheroids. Third, it is much more accurate for low aspect ratio, sphere-like particles (Fig. 2). A noticeable discrepancy between all of these approximations and the rigorous T-matrix solution is the presence of extra resonances in-between the longitudinal and transverse resonance of the high-aspect ratio spheroids (Fig. 1, $\lambda \sim 500$ nm). This is expected because these resonances are associated with higher multipoles, such as quadrupole and octupole, while the previously described approximations only apply to the dipolar response. Other higher-order multipolar resonances are also likely superimposed in the spectral region of the transverse resonance and could explain the larger discrepancies observed there. We will now show how these resonances can be simply included within the same framework of the Taylor approximation obtained from a T-matrix.

III. QUADRUPOLE AND HIGHER ORDER RESONANCES

While the Taylor dipolar terms are accurate enough for many practical applications in plasmonics, the series expansion of the far field to $\mathcal{O}(X^6)$ also includes a range of higher order multipole contributions, and for sufficiently large particles, these terms can have a noticeable presence in the optical response. These multipolar terms were also derived in Ref. 24 from the T-matrix solution, and they provide an intuitive understanding of how the scattered field is constructed in the long-wavelength limit. We briefly summarize the T-matrix method, and what physical meaning is attached to the matrix elements.[16] In the T-matrix formalism, the basis elements of the electromagnetic fields are the electric and magnetic multipoles. The fields are expressed as series of multipolar components, and each T-matrix element $T^{ij}_{nk|m}$ denotes how a particular multipole of degree n and order m (orientation) responds to excitation by an external multipole of degree k and order m (for spheroids, there is no coupling between different m values). The superscripts ij indicate whether the incident (j) or induced (i) multipoles are of the electric ($i,j = 2$) or magnetic ($i,j = 1$) type. For instance, $T^{22}_{11|0}$ is the magnitude of the electric dipole induced by the electric dipole component of the incident field, oriented along z ($m = 0$). This is effectively the polarizability α_z up to a normalization factor. Usually, in plasmonics, the particles are non-magnetic, so the more significant interactions are between electric multipoles or the $T^{22}_{nk|m}$ elements, especially in the low frequency/small particle limit.

The orientation-averaged extinction cross section is obtained from the trace of the T-matrix. The only terms of order X^6 or less in this sum are the electric dipole interactions $T^{22}_{11|m}$, magnetic dipole interactions $T^{11}_{11|m}$, and electric quadrupole interactions $T^{22}_{22|m}$, and we have

$$\langle C_{\text{ext}}\rangle = \frac{-2\pi}{k_1^2}\mathrm{Re}\Big\{T^{11}_{11|0} + T^{22}_{11|0} + T^{22}_{22|0} + 2\big[T^{11}_{11|1} + T^{22}_{11|1} + T^{22}_{22|1} + T^{22}_{22|2}\big]\Big\} + \mathcal{O}(X^7). \tag{20}$$

The orientation-averaged scattering cross section is computed similarly from the sum of the squares of all elements of the T-matrix. To $\mathcal{O}(X^6)$, there are 11 independent non-zero matrix elements,

$$\langle C_{\text{sca}}\rangle = \frac{2\pi}{k_1^2}\Big\{|T^{11}_{11|0}|^2 + |T^{22}_{11|0}|^2 + |T^{22}_{22|0}|^2 + 2|T^{22}_{31|0}|^2 + 2|T^{11}_{11|1}|^2 + 2|T^{22}_{11|1}|^2 + 4|T^{21}_{12|1}|^2 + 4|T^{21}_{21|1}|^2 + 4|T^{22}_{31|1}|^2 + 2|T^{22}_{22|1}|^2 + 2|T^{22}_{22|2}|^2\Big\} + \mathcal{O}(X^{10}). \tag{21}$$

Note that this expression is only correct up to order $O(X^9)$, i.e., the error is of order $O(X^{10})$, because the dipole terms will have terms of this order that are not accounted for within the approximation of Eq. (5). In fact, all but the first two dipolar elements are also of order X^{10} themselves so could, in principle, be ignored, but we have included them because they have resonances in different parts of the spectrum and may become important in regions where the dipole terms are small, as shown in Fig. 6 in Appendix B. The lowest order approximations for all matrix elements were derived in Ref. 24, including their radiative corrections. For convenience, the expressions are summarized in Appendix C. A Matlab function is also provided as the supplementary material, to evaluate these cross sections for any input size, shape, dielectric function, and frequency.

Figure 3 shows the individual contribution to the extinction spectra of all the matrix elements [correct to $\mathcal{O}(X^6)$] for two

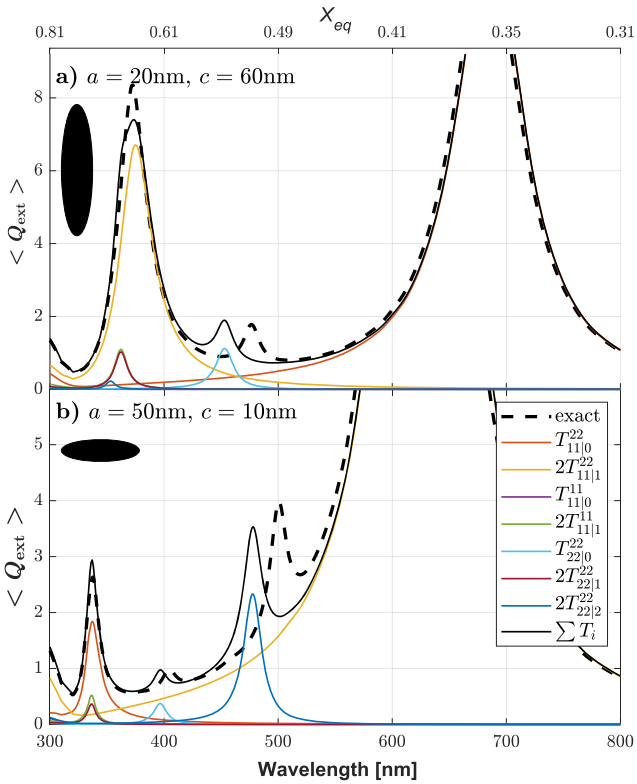

FIG. 3. Individual contributions from each T-matrix element in the sum to obtain the approximate orientation-averaged extinction spectrum [Eq. (18)] for a representative prolate (a) and oblate (b) silver spheroid in water. The sum of these terms [Eq. (18)] is also shown as a black solid line and the rigorous T-matrix solution as a dashed line. The wavelength-dependent size parameter X_{eq} is approximately the same for both and given on the top x-axis.

example prolate and oblate silver spheroids in water. In plasmonics, the electric quadrupole excitations $T^{22}_{22|m}$ tend to be the leading higher order corrections.[44] There are three quadrupole moments that may be excited for $m = 0, 1, 2$, and each has their own resonant frequency. The magnetic dipole term $T^{11}_{11|1}$ also has a resonance similar to $T^{22}_{22|1}$. The contribution of $T^{11}_{11|0}$ is negligible as it has no resonance at this order. We note that the Fröhlich frequency of these higher-order resonances tends to be near the dipolar x resonance, so what may appear as simply a dipole resonance is actually a sum of different orders, where these higher-order contributions enhance and/or spread the peak and may interfere. Including these higher-order terms results in an improved agreement with the exact results, but some discrepancies remain. Notably, the exact high-order resonances are redshifted compared to our approximate expressions (but the correct strength is predicted). This discrepancy is caused by a similar retardation effect as observed for the electrostatic dipole resonance. This shift could, in principle, be corrected by including the next order correction $[\mathcal{O}(X^7)]$, although it could be a difficult task to determine it analytically. Nevertheless, the approximation provides a practical means to interpret the origin of each resonance peak. For example, the longest wavelength quadrupole peak can be attributed to $m = 0$ for the prolate spheroid but to $m = 2$ for the oblate spheroid. A similar analysis can be carried out for the scattering spectrum, but the four additional terms appearing in its expression are negligible for the chosen parameters and are not discussed further here. In addition, we can note that for gold, the higher-order resonances are much less pronounced due to the high losses in that spectral region, which explains the relatively better agreement with predictions of the dipolar approximation (see Appendix A).

Finally, it is worth highlighting that in the small size limit, the resonances of the T-matrix elements generally occur when $1 + (\varepsilon(\omega) - 1)L^m_n = 0$, where L^m_n are generalized multipole depolarization factors.[45–48] For dipoles, they reduce to the well-known expressions $L^0_1 = L_z$, $L^1_1 = L_x = L_y$, (3) and (4), while for quadrupoles, L^0_2, L^1_2, L^2_2 are given in Appendix C. These expressions could be used for a further analytical description of these resonances.

IV. CONCLUSION

We have shown that the recently derived exact Taylor expansion of the T-matrix solution[24] provides a simple approach to compute the orientation-averaged optical spectra of metallic spheroidal nanoparticles. For the dipolar resonances/polarizabilities, the approximation has the same functional form [Eq. (5)] as in previous studies, such as those based on the MLWA, but uses a different expression for the dynamic correction term. It provides a better approximation for both oblate and prolate spheroids over a wider range of material and geometric parameters. It also provides a simple means to include and study the effect of higher-order resonances. This approximation will therefore be useful for a routine comparison with experiments and for further theoretical developments where the full exact solution is too complex to be handled analytically.

SUPPLEMENTARY MATERIAL

See supplementary material for an example Matlab function `getTmatrixApprox.m`, which computes the approximate T-matrix elements and derived optical properties.

ACKNOWLEDGMENTS

The authors acknowledge financial support from the a Whitinga fellowship (M.R.A.M.), and a Rutherford Discovery Fellowship (B.A.), and the Marsden Grant of the Royal Society New Zealand (E.C.L.R.).

AUTHOR DECLARATIONS

Conflict of Interest

The authors have no conflicts to disclose.

DATA AVAILABILITY

The data that support the findings of this study are available from the corresponding author upon reasonable request. The Matlab code supplied as the supplementary material can also be used to reproduce the predictions of the Taylor approximation.

APPENDIX A: FIGURES FOR GOLD SPHEROIDS IN WATER

The equivalent of Figs. 1 and 2 but for gold instead of silver are presented in Figs. 4 and 5. The gold dielectric function is taken from Ref. 49 (SC data).

APPENDIX B: FIGURE FOR SCATTERING CROSS SECTION

The equivalent of Fig. 3, but for the scattering cross section, is presented in Fig. 6.

APPENDIX C: EXPLICIT EXPRESSIONS FOR MATRIX ELEMENTS

Following Ref. 24, to account for the radiative correction, the T-matrix elements are expressed in terms of the K matrix with $\mathbf{T} = i\mathbf{K}(\mathbf{I} - i\mathbf{K})^{-1}$. All expressions for matrix elements below are correct to $\mathcal{O}(X^6)$.

For $m = 0$, we have

$$T^{11}_{11|0} = \frac{iK^{11}_{11|0}}{1 - iK^{11}_{11|0}}, \tag{C1}$$

$$T^{22}_{22|0} = \frac{iK^{22}_{22|0}}{1 - iK^{22}_{22|0}}, \tag{C2}$$

$$T^{22}_{11|0} = \frac{iK_0X^3}{1 - \Omega_0X^2 - iK_0X^3}, \tag{C3}$$

$$T^{22}_{31|0} = T^{22}_{13|0} = \frac{i\frac{\sqrt{14}e^2}{175}K_0X^5}{1 - \Omega_0X^2 - iK_0X^3}, \tag{C4}$$

where Ω_0 is given in Eq. (14) and K_0 is related to the static dipolar polarizability along the z axis, α_{zz},

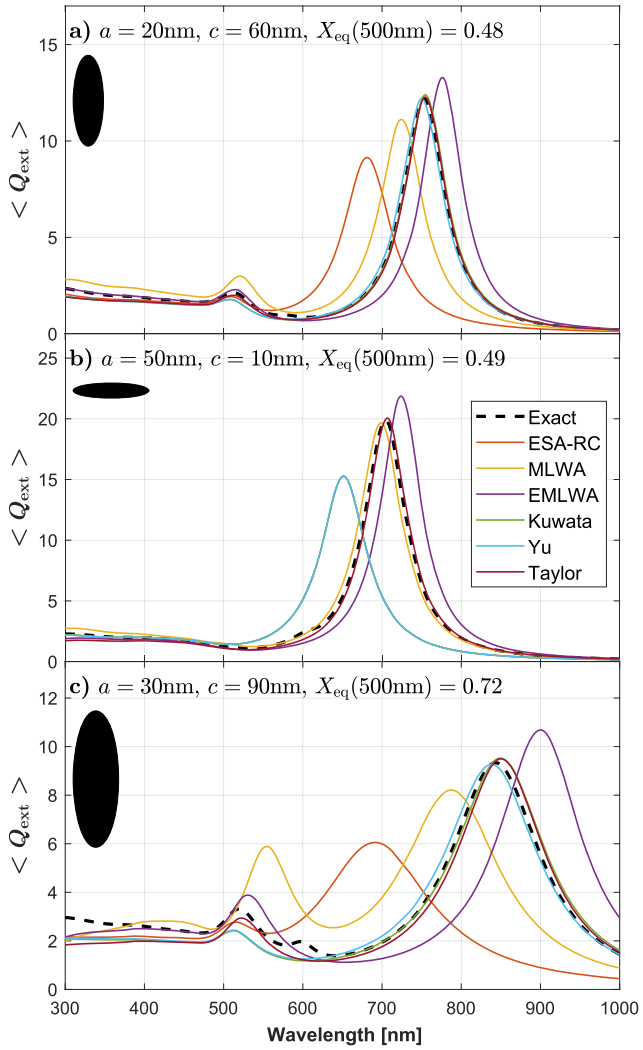

FIG. 4. Extinction coefficient spectra for gold spheroids of high aspect ratios calculated from the various approximations: (a) 40 × 120 nm^2 prolate, (b) 100 × 20 nm^2 oblate, and (c) 60 × 180 nm^2 prolate. The rigorous T-matrix reference solution is plotted as a dashed line.

$$K_0 = \frac{2}{9h^2}\frac{s^2-1}{1+(s^2-1)L_z} = \frac{2}{3c^3}\frac{\alpha_{zz}}{4\pi\varepsilon_1}, \tag{C5}$$

where $h = c/a$ is the aspect ratio, $e = \sqrt{1-1/h^2}$ is the eccentricity (imaginary for oblate spheroids), s is the relative refractive index ($s^2 = \varepsilon$), and L_z is given in Eq. (3). The K-matrix elements are

$$K^{22}_{13|0} = K^{22}_{31|0} = \frac{2e^2\sqrt{14}}{1575h^2}\frac{s^2-1}{1+(s^2-1)L_z}X^5, \tag{C6}$$

$$K^{11}_{11|0} = \frac{s^2-1}{45h^4}X^5, \tag{C7}$$

$$K^{22}_{22|0} = \frac{3-e^2}{225h^2}\frac{s^2-1}{1+(s^2-1)L^0_2}X^5, \tag{C8}$$

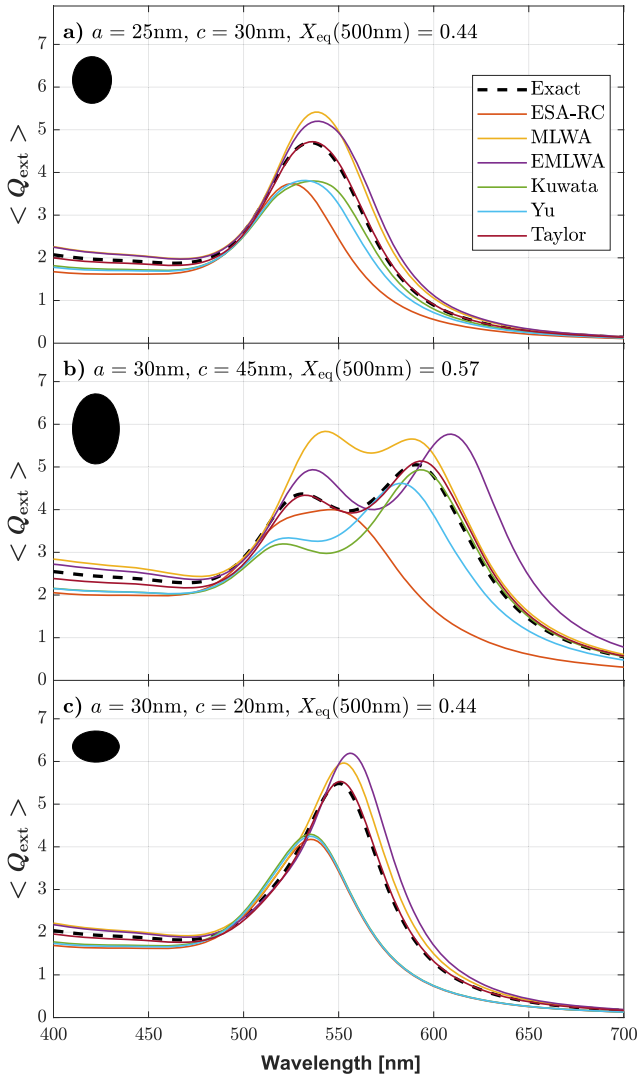

FIG. 5. Extinction coefficient spectra for gold spheroids of low aspect ratios calculated from the various approximations: (a) 50 × 60 nm^2 prolate, (b) 60 × 90 nm^2 prolate, and (c) 60 × 40 nm^2 oblate. The rigorous T-matrix reference solution is plotted as a dashed line.

with

$$L^0_2 = \frac{3}{2}\frac{1-e^2}{e^3}\left[\frac{3-e^2}{e^2}\operatorname{atanh}(e) - \frac{3}{e}\right]. \tag{C9}$$

For $m = 1$, we have

$$T^{11}_{11|1} = \frac{iK^{11}_{11|1}}{1-i\left[K^{11}_{11|1} - (K^{21}_{21|1})^2/K^{11}_{11|1}\right]}, \tag{C10}$$

$$T^{22}_{22|1} = \frac{iK^{22}_{22|1}}{1-i\left[K^{22}_{22|1} - (K^{21}_{21|1})^2/K^{22}_{22|1}\right]}, \tag{C11}$$

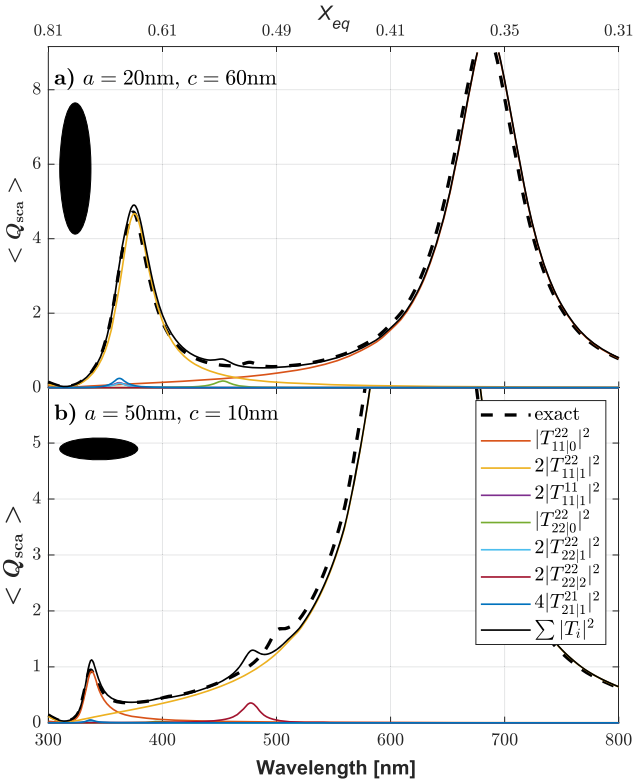

FIG. 6. Individual contributions from each T-matrix element in the sum to obtain the approximate orientation-averaged scattering spectrum [Eq. (19)] for a representative prolate (a) and oblate (b) silver spheroid in water. The sum of these terms [Eq. (19)] is also shown as a black solid line and the rigorous T-matrix solution as a dashed line. Some terms from Eq. (19) are negligible and not shown.

$$T^{21}_{21|1} = -T^{12}_{12|1} = \frac{iK^{21}_{21|1}}{1 - i\left[K^{11}_{11|1} + K^{22}_{22|1}\right]}, \tag{C12}$$

$$T^{22}_{11|1} = \frac{iK_1X^3}{1 - \Omega_1X^2 - iK_1X^3}, \tag{C13}$$

$$T^{21}_{12|1} = -T^{12}_{21|1} = \frac{iK^{21}_{12|1}}{1 - iK_1X^3}, \tag{C14}$$

$$T^{22}_{31|1} = T^{22}_{13|1} = \frac{iK^{22}_{31|1}}{1 - iK_1X^3}. \tag{C15}$$

Ω_1 is given in Eq. (15) and K_1 is related to the static dipolar polarizability along the x or y axis, $\alpha_{xx} = \alpha_{yy}$,

$$K_1 = \frac{2}{9h^2}\frac{s^2 - 1}{1 + (s^2 - 1)L_x} = \frac{2}{3c^3}\frac{\alpha_{xx}}{4\pi\varepsilon_1}, \tag{C16}$$

where L_x is given in Eq. (4). The K-matrix elements are

$$K^{22}_{11|1} = \frac{K_1X^3}{1 - \Omega_1X^3}, \tag{C17}$$

$$K^{22}_{13|1} = K^{22}_{31|1} = \frac{2e^2\sqrt{21}}{525}K_1X^5, \tag{C18}$$

$$K^{21}_{12|1} = -K^{12}_{21|1} = \frac{ie^2\sqrt{15}}{150}K_1X^5, \tag{C19}$$

$$K^{11}_{11|1} = \frac{(s^2 - 1)\left[h^2(2 - e^2)^2 + 4(s^2 - 1)L^1_2\right]}{90h^4(2 - e^2)\left[1 + (s^2 - 1)L^1_2\right]}X^5, \tag{C20}$$

$$K^{22}_{22|1} = \frac{2 - e^2}{150h^2}\frac{s^2 - 1}{1 + (s^2 - 1)L^1_2}X^5, \tag{C21}$$

$$K^{21}_{21|1} = -K^{12}_{12|1} = \frac{ie^2X^5}{30\sqrt{15}h^2}\frac{s^2 - 1}{1 + (s^2 - 1)L^1_2}, \tag{C22}$$

with

$$L^1_2 = -\frac{2 - e^2}{2e^4}\left[3\frac{1 - e^2}{e}\text{atanh}(e) - 3 + 2e^2\right]. \tag{C23}$$

Finally, for $m = 2$, we have

$$T^{22}_{22|2} = \frac{iK^{22}_{22|2}}{1 - iK^{22}_{22|2}}, \tag{C24}$$

with

$$K^{22}_{22|2} = \frac{X^5}{75h^4}\frac{s^2 - 1}{1 + (s^2 - 1)L^2_2} \tag{C25}$$

and

$$L^2_2 = \frac{1}{4e^4}\left[\frac{3}{e}(1 - e^2)^2\text{atanh}(e) - 3 + 5e^2\right]. \tag{C26}$$

REFERENCES

[1] K. A. Willets and R. P. Van Duyne, "Localized surface plasmon resonance spectroscopy and sensing," Annu. Rev. Phys. Chem. **58**(1), 267–297 (2007).
[2] E. C. Le Ru and P. G. Etchegoin, *Principles of Surface Enhanced Raman Spectroscopy and Related Plasmonic Effects* (Elsevier, Amsterdam, 2009).
[3] J. Langer *et al.*, "Present and future of surface-enhanced Raman scattering," ACS Nano **14**, 28–117 (2020).
[4] X. X. Han, R. S. Rodriguez, C. L. Haynes, Y. Ozaki, and B. Zhao, "Modified optical absorption of molecules on metallic nanoparticles at sub-monolayer coverage," Nat. Rev. Methods Primers **1**(1), 87 (2022).
[5] G. Zengin, T. Gschneidtner, R. Verre, L. Shao, T. J. Antosiewicz, K. Moth-Poulsen, M. Käll, and T. Shegai, "Evaluating conditions for strong coupling between nanoparticle plasmons and organic dyes using scattering and absorption spectroscopy," J. Phys. Chem. C **120**(37), 20588–20596 (2016).
[6] R. Chikkaraddy, B. de Nijs, F. Benz, S. J. Barrow, O. A. Scherman, E. Rosta, A. Demetriadou, P. Fox, O. Hess, and J. J. Baumberg, "Single-molecule strong coupling at room temperature in plasmonic nanocavities," Nature **535**(7610), 127 (2016).
[7] B. L. Darby, B. Auguié, M. Meyer, A. E. Pantoja, and E. C. Le Ru, "Modified optical absorption of molecules on metallic nanoparticles at sub-monolayer coverage," Nat. Photonics **10**(1), 40 (2016).
[8] T. E. Tesema, H. Kookhaee, and T. G. Habteyes, "Extracting electronic transition bands of adsorbates from molecule–plasmon excitation coupling," J. Phys. Chem. Lett. **11**(9), 3507–3514 (2020).
[9] A. Politano, A. Cupolillo, G. Di Profio, H. A. Arafat, G. Chiarello, and E. Curcio, "When plasmonics meets membrane technology," J. Phys.: Condens. Matter **28**(36), 363003 (2016).
[10] C. Clavero, "Plasmon-induced hot-electron generation at nanoparticle/metal-oxide interfaces for photovoltaic and photocatalytic devices," Nat. Photonics **8**(2), 95–103 (2014).

[11] B. Gallinet, J. Butet, O. J. F. Martin, "Numerical methods for nanophotonics: Standard problems and future challenges," Laser Photonics Rev. **9**(6), 577–603 (2015).
[12] M. Yurkin, "Computational approaches for plasmonics," in *Handbook of Molecular Plasmonics*, edited by S. D'Agostino (Pan Stanford Publishing, 2013), pp. 83–135.
[13] A. M. Kern and O. J. F. Martin, "Surface integral formulation for 3D simulations of plasmonic and high permittivity nanostructures," J. Opt. Soc. Am. A **26**(4), 732–740 (2009).
[14] T. V. Raziman, W. R. C. Somerville, O. J. F. Martin, and E. C. Le Ru, "Accuracy of surface integral equation matrix elements in plasmonic calculations," J. Opt. Soc. Am. B **32**(3), 485–492 (2015).
[15] J. Grand and E. C. Le Ru, "Practical implementation of accurate finite-element calculations for electromagnetic scattering by nanoparticles," Plasmonics **15**(1), 109–121 (2020).
[16] M. I. Mishchenko, L. D. Travis, and A. A. Lacis, *Scattering, Absorption, and Emission of Light by Small Particles*, 3rd ed. (Cambridge University Press, Cambridge, 2002).
[17] W. R. C. Somerville, B. Auguié, and E. C. Le Ru, "Accurate and convergent T-matrix calculations of light scattering by spheroids," J. Quant. Spectrosc. Radiat. Transfer **160**, 29–35 (2015).
[18] C. F. Bohren and D. R. Huffman, *Absorption and Scattering of Light by Small Particles* (Wiley, 1983).
[19] M. Meier and A. Wokaun, "Enhanced fields on large metal particles: Dynamic depolarization," Opt. Lett. **8**(11), 581–583 (1983).
[20] K. L. Kelly, E. Coronado, L. L. Zhao, and G. C. Schatz, "The optical properties of metal nanoparticles: The influence of size, shape, and dielectric environment," J. Phys. Chem. B **107**, 668–677 (2003).
[21] A. Moroz, "Depolarization field of spheroidal particles," J.Opt. Soc. Am. B **26**(3), 517–527 (2009).
[22] H. Kuwata, H. Tamaru, K. Esumi, and K. Miyano, "Resonant light scattering from metal nanoparticles: Practical analysis beyond Rayleigh approximation," Appl. Phys. Lett. **83**(22), 4625–4627 (2003).
[23] D. Schebarchov, B. Auguié, and E. C. Le Ru, "Simple accurate approximations for the optical properties of metallic nanospheres and nanoshells," Phys. Chem. Chem. Phys. **15**(12), 4233–4242 (2013).
[24] M. Majic, L. Pratley, D. Schebarchov, W. R. Somerville, B. Auguié, and E. C. Le Ru, "Approximate *T*-matrix and optical properties of spheroidal particles to third order with respect to size parameter," Phys. Rev. A **99**(1), 013853 (2019).
[25] M. Januar, B. Liu, J.-C. Cheng, K. Hatanaka, H. Misawa, H.-H. Hsiao, and K.-C. Liu, "Role of depolarization factors in the evolution of a dipolar plasmonic spectral line in the far-and near-field regimes," J. Phys. Chem. C **124**(5), 3250–3259 (2020).
[26] I. L. Rasskazov, V. I. Zakomirnyi, A. D. Utyushev, P. S. Carney, and A. Moroz, "Remarkable predictive power of the modified long wavelength approximation," J. Phys. Chem. C **125**(3), 1963–1971 (2021).
[27] A. F. Stevenson, "Electromagnetic scattering by an ellipsoid in the third approximation," J. Appl. Phys. **24**(9), 1143–1151 (1953).
[28] R. Yu, L. M. Liz-Marzán, and F. J. García de Abajo, "Universal analytical modeling of plasmonic nanoparticles," Chem. Soc. Rev. **46**, 6710–6724 (2017).
[29] H. Y. Chung, P. T. Leung, and D. P. Tsai, "Dynamic modifications of polarizability for large metallic spheroidal nanoshells," J. Chem. Phys. **131**(12), 124122 (2009).
[30] V. Grigoriev, N. Bonod, J. Wenger, and B. Stout, "Optimizing nanoparticle designs for ideal absorption of light," ACS Photonics **2**(2), 263–270 (2015).
[31] Y. Wu, Z. Hu, X.-T. Kong, J. C. Idrobo, A. G. Nixon, P. D. Rack, D. J. Masiello, and J. P. Camden, "Infrared plasmonics: STEM-EELS characterization of Fabry-Pérot resonance damping in gold nanowires," Phys. Rev. B **101**(8), 085409 (2020).
[32] A. L. Schmucker, N. Harris, M. J. Banholzer, M. G. Blaber, K. D. Osberg, G. C. Schatz, and C. A. Mirkin, "Correlating nanorod structure with experimentally measured and theoretically predicted surface plasmon resonance," ACS Nano **4**(9), 5453–5463 (2010).
[33] I. Zoric, M. Zach, B. Kasemo, and C. Langhammer, "Gold, platinum, and aluminum nanodisk plasmons: Material independence, subradiance, and damping mechanisms," ACS Nano **5**(4), 2535–2546 (2011).
[34] N. G. Khlebtsov and E. C. Le Ru, "Analytical solutions for the surface- and orientation-averaged SERS enhancement factor of small plasmonic particles," J. Raman Spectrosc. **52**, 285–295 (2021).
[35] N. G. Khlebtsov, "Extinction and scattering of light by nonspherical plasmonic particles in absorbing media," J. Quant. Spectrosc. Radiat. Transfer **280**, 108069 (2022).
[36] P. Barber and C. Yeh, "Scattering of electromagnetic waves by arbitrarily shaped dielectric bodies," Appl. Opt. **14**(12), 2864–2872 (1975).
[37] W. R. C. Somerville, B. Auguié, and E. C. Le Ru, "Severe loss of precision in calculations of *T*-matrix integrals," J. Quant. Spectrosc. Radiat. Transfer **113**(7), 524–535 (2012).
[38] E. C. Le Ru, W. R. C. Somerville, and B. Auguié, "Radiative correction in approximate treatments of electromagnetic scattering by point and body scatterers," Phys. Rev. A **87**(1), 012504 (2013).
[39] E. J. Zeman and G. C. Schatz, "An accurate electromagnetic theory study of surface enhancement factors for silver, gold, copper, lithium, sodium, aluminum, gallium, indium, zinc, and cadmium," J. Phys. Chem. **91**(3), 634–643 (1987).
[40] A. E. Moskalensky and M. A. Yurkin, "Energy budget and optical theorem for scattering of source-induced fields," Phys. Rev. A **99**(5), 053824 (2019).
[41] A. E. Moskalensky and M. A. Yurkin, "A point electric dipole: From basic optical properties to the fluctuation–dissipation theorem," Rev. Phys. **6**, 100047 (2021).
[42] W. R. C. Somerville, B. Auguié, and E. C. Le Ru, "SMARTIES: User-friendly codes for fast and accurate calculations of light scattering by spheroids," J. Quant. Spectrosc. Radiat. Transfer **174**, 39–55 (2016).
[43] H. U. Yang, J. D'Archangel, M. L. Sundheimer, E. Tucker, G. D. Boreman, and M. B. Raschke, "Optical dielectric function of silver," Phys. Rev. B **91**, 235137 (2015).
[44] U. Kreibig and M. Vollmer, "Optical properties of metal clusters," in *Material Science* (Springer, 1995).
[45] J. C. E. Sten, "Multiline singularities applied to low-frequency scattering by a prolate spheroid," Compel **16**(2), 92–107 (1997).
[46] R. C. Voicu and T. Sandu, "Analytical results regarding electrostatic resonances of surface phonon/plasmon polaritons: Separation of variables with a twist," Proc. R. Soc. A **473**(2199), 20160796 (2017).
[47] M. Majic, F. Gray, B. Auguié, and E. C. Le Ru, "Electrostatic limit of the *T*-matrix for electromagnetic scattering: Exact results for spheroidal particles," J. Quant. Spectrosc. Radiat. Transfer **200**, 50–58 (2017).
[48] M. Majic and E. C. Le Ru, "Quasistatic limit of the electric-magnetic coupling blocks of the *T*-matrix for spheroids," J. Quant. Spectrosc. Radiat. Transfer **225**, 16–24 (2019).
[49] R. L. Olmon, B. Slovick, T. W. Johnson, D. Shelton, S.-H. Oh, G. D. Boreman, and M. B. Raschke, "Optical dielectric function of gold," Phys. Rev. B **86**, 235147 (2012).